The 2013 World Congress on
Advances in Structural Engineering and Mechanics (ASEM13)
Jeju, Korea, September 8-12, 2013

Innovative Post-tensioned Hybrid Wind Turbine Tower Made of Ultra High Performance Cementitious Composites Segment

*Xiang-Guo Wu[1)] Jiang Yang[2)] and Issa Brown Mpalla [3)]

[1), 2), 3)] *School of Civil Engineering, Harbin Institute of Technology, Harbin 150001, China*

[1)] wuxiangguo@hit.edu.cn [2)] yangjing0639@163.com [3)] issabrownm@yahoo.co.uk

ABSTRACT

Ultra High Performance Cementitious Composites with compressive strength 200MPa (UHPCC-200) is proposed for the structural design of super high hybrid wind turbine tower to gain durability, ductility and high strength design objectives. The minimal wall thickness is analyzed using basic bending and compression theory and is modified by a toque influence coefficient. Two cases of wall thickness combination of middle and bottom segment including varied ratio and constant ratio are considered within typical wall thickness dimension. Using nonlinear finite element analysis, the effects of wall thickness combinations with varied and constant ratio and prestress on the structural stress and lateral displacement are calculated and analyzed. The design limitation of the segmental wall thickness combinations is recommended.

1. INTRODUCTION

As the support component of a wind turbine system, wind turbine tower is used to lift the sails at design height ensuring the wind turbine to gain stable wind resources. Enough strength, stiffness and stability are required for the support component (Zhang 2009). Utility-scale wind farm development has been underway for approximately three decades, and in that time, the tower structural systems (for supporting large wind turbines) have changed dramatically—from relatively short 20m to 40 m steel lattice towers and guyed or self-supporting poles, to moderately tall 40 m to 60 m thin-shell steel fabricated tubes, and to the current wind industry standard of taller 80 m to 100 m steel fabricated tubes(Nestor and Rolando 2012). Recent years, ultrahigh wind turbine tower i.e. over one hundred meters height is one important developing trend for MW degree wind turbine system to gain more stable wind speed. However, the section diameter of the super high steel tower will greater than highway transportation limit of 4.2m. Developing hybrid tower is an innovative selection to solve the highway transportation difficulty. Additionally, utilization of durable engineering material is an effective for realization of high durable infrastructure. Based on the aforementioned background and the conception of Advanced Wind Turbine System (ATS) (The Concrete Centre 2007; Eize 2009; Brughis 2004), Ultra High Performance

[1)] Associate professor

Cementitious Composites (UHPCC) is proposed for the super high and durable wind turbine tower design.

As a new generation of engineering infrastructure material, UHPCC exhibits high strength and durable properties. Recently, a number of researchers have carried out extensive researches and engaged in international communication in the areas of material properties, and UHPCC hybrid elements (Wu et al. 2010). Some new types of bridge member employing UHPCC were applied such as Shepherds Creek Bridge in Australia (Cavill et al. 2003), Wapello Bridge in Iowa, USA (Graybeal et al. 2004), Kuyshu High Speed Bridge in Japan (Okuma 2006), FHWA short span bridge in the USA (Graybeal et al. 2004), the Saint-Pierre-La-Cour hybrid bridge in France (Behloul 2007), and UHPCC permanent form in China(Wu et al. 2012). By now, there has no report about the application study of UHPCC in hybrid super high tower.

In super high UHPCC hybrid tower preliminary design, segmental wall thickness and wall thickness ratio between middle part and bottom part are important parameters for the structural overall design. The general design proposal of the UHPCC hybrid tower is described firstly. The effects of segmental wall thickness combinations and prestressing force on structural overall behavior under ultimate load model are analyzed using nonlinear finite element.

2. OUTLINE OF UHPCC PROPERTIES

UHPCC with compressive strength 200MPa is proposed for durable hybrid tower and the material is noted as UHPCC-200 in this paper. Properties of UHPCC-200 including mixing compositions, mechanical and durability properties are introduced briefly. More detail information and its constitutive model can be referenced from properties introductions of UHPCC (Williams et al. 2010, Ramadoss et al. 2008, and Kittinun et al. 2010).

2.1 Mixing compositions of UHPCC-200

Mixing compositions of UHPCC-200 are shown in Table 1. Fine silica sand is substituted by normal sand from the Songhua River to reduce the material cost. The steel fiber mixing content is 2% of the composites.

Table 1 Mixing compositions of UHPCC-200 (kg/m3)

Cement	Silica fume	Filling powder	Fine sand	Super Plast.	Water	Expan. agent	Defoamer	Steel fiber
798.45	213.43	161.56	864.74	33.48	164.71	3.95	3.95	108.36

2.2 Mechanics behavior of UHPCC

The design tensile strength of the material for the hybrid tower is 15MPa. For simplification and conservative analysis, the design cracking strength of the material is 6MPa. Strain hardening is omitted in this analysis. The simplified model of UHPCC proposed by FHWA (Federal High Way Administration of America)(Benjamin 2006) is used as shown in figure 1. Corresponding parameters values are listed in Table 2.

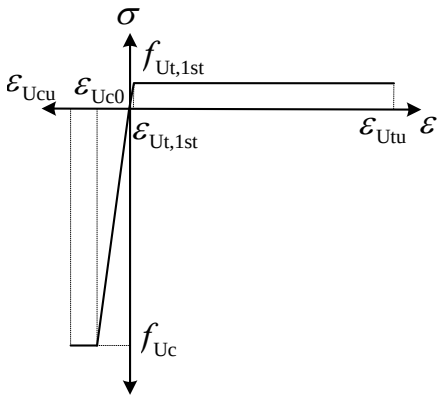

Fig. 1 Simplified stress-strain model of UHPCC

Table 2 Parameters of UHPCC simplified constitutive model

Parameter	Cracking strength	The first tensile cracking strain	Ultimate tensile strength	Ultimate tensile strain	Elastic Modulus	Poisson's ratio	Compressive strength	Ultimate compressive strain
Value	6MPa	0.0001	15MPa	0.0025	45GPa	0.18	200	0.0036

2.3 Durability of UHPCC-200

Durability of segment material will determine the overall durability of the infracture. The design objective of UHPCC for the hybrid tower include the resistance ability to chloride attack, resistance to freezing-thawing etc. Table 3 shows the design indexes of UHPCC-200 for the hybrid tower with comparisons with NSC and HSC/HPC (high strength concrete/high performance concrete). And these design indexes are within the normal durability levels of UHPCC.

Table 3 Durability Comparison of UHPCC with NSC and HSC/HPC

Property		NSC	HSC/HPC	UHPCC-200	Measurement
Resistance of Chloride attack (Coulombs)		2,445	178	2.0	ASTM C 1202
Neutralization (depth: mm, 6 month)		17	3.5	0	CO2 10%, RH 60%, 30℃
Resistance of Freezing-Thawing (Relative Dynamic Elastic Modulus: %, 600 cycles)		78	95	100	ASTM C 666 B
Permeability	Air permeability (X10-16m2)	0.1335	0.0475	0.01	Direct Pressure
	Water Permeability (mm2/sec·Bar)	0.00362	0.00259	0.0004	
	Permeability (Coulombs)	776	135	1.0	ASTM C 1202
Porosity (ml/g)		0.1605	0.0874	0.05	Auto Pore 9220

3. INNOVATIVE DESIGN OUTLINES OF THE HYBRID TOWER

The design objective of this hybrid tower is to support 3MW wind turbine system and its main technical parameters are listed in Table 4 (Staffan et al. 2010). The tower is divided into three parts, i.e. upper steel cylinder part, middle and bottom UHPCC taper cylinder parts as shown in figure 2.

The height of the upper steel part is 2m and its wall thickness is 20mm. The middle and bottom parts are constructed by prefabricated UHPCC segments and the total height of these two parts is 118m. The middle part is connected with the upper steel cylinder part. The initial design thickness of the middle part segment thickness is in the scope of 100mm ~ 200mm. The design height of the bottom taper cylinder is 20m and its initial thickness is in the scope of 150mm ~ 300mm. To satisfy highway transportation requirement, the middle and bottom UHPCC parts are separated into several UHPCC longitudinal prefabricate segments. The segments are connected by external prestressing tendon as shown in figure 3. Adjacent segments are connected

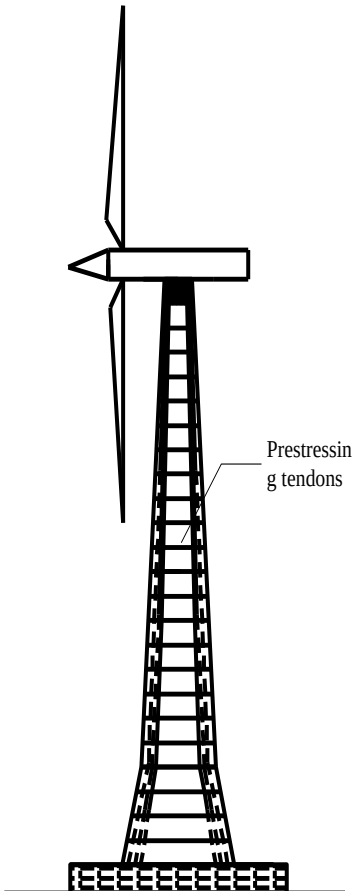

(a) Three parts and segment (b) Prestressing tendon

Fig.2 UHPCC hybrid tower

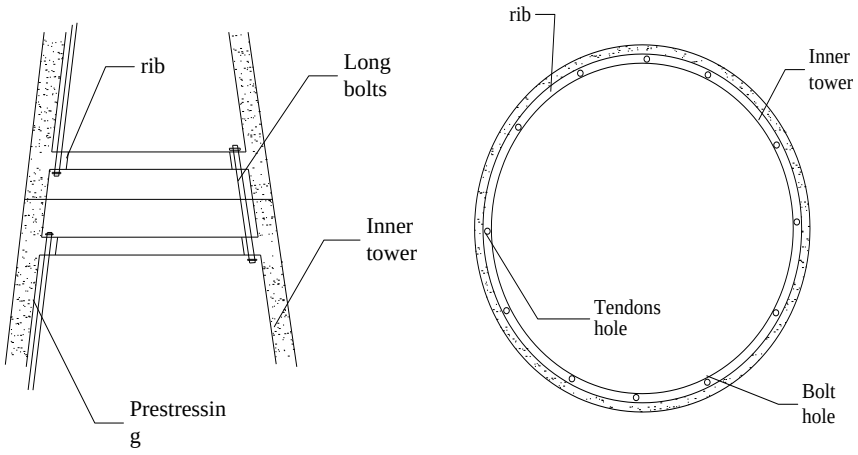

(a) Bolt connection (b) Segment cross section

Fig.3 Local detailed diagram

with interval flexible bolts. The three parts are perforated overall using external prestressing tendon from the top to the base. The top and bottom of each UHPCC segment element are arranged with one ring rib which is used for the arrangement of prestressing tendon and bolt connection. The design diameter of the tower base and top are 12m and 3m, respectively. Every hole is arranged with six tendons and eight holes on every ring rib are arranged with tendons. Total 48 tendons are used here. Other four holes are arranged with bolt connections.

Table 4 Main parameter of wind turbine

Rated Power	3MW	number of blade	3
Rated wind of height V at wheel hub	13.5 m/s	cut-in wind speed	3.5 m/s
power control mode	variable speed adjustable pitch	cut-out speed	25 m/s
Unit safe level	IEC IB	rotor speed	9-17rpm
hub height	123m	Sweep area	7850 m^2
rotor diameter R	100m	main-shaft tilt angle	7°
Impeller weight G_1	85 t	Cabin weight G_2	127 t

4. LOAD MODEL AND PARAMETERS

4.1 Top concentrated load

The tower can be simplified as a variable cross-sectional cantilever beam with longitudinal distributed load, top concentrated load such as the self weight of engine room, hub, lamina and the top moment due to the concentrated load eccentricity.

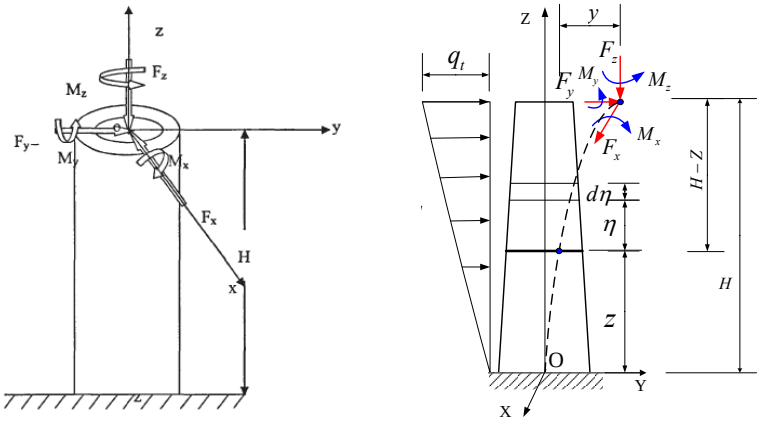

(a) Top concentrated loads (b) Mechanical model

Fig.4 The coordinate system of tower top upper surface

The original point is defined as the intersection point of tower axis and top upper surface as shown in Fig. 4(a) in which X is the direction along the axis of wind wheel, Z is the normal direction of the upper surface, and Y is the direction determined by right hand rule. Here, F_x is aerodynamic thrust on wind wheel, F_y is pulsating force on laminas, F_z is the tower axial compressive force, M_x is the pitching moment due to wind wheel and engine, M_y is the pitching moment resulted from gradient, M_z is the torsion from wind wheel. The calculation formula of F_x, F_y, F_z, M_x, M_y and M_z can be referenced from Zhang 2009. Wind speed *V* at height of H can be written as

$$\frac{V}{V_0}=\left(\frac{H}{H_0}\right)^{\alpha} \tag{1}$$

In which, V_0 is wind speed value at height of H_0 usually selected as 10m from ground (m/s). α is the wind shear coefficient located between 0.1 and 0.4. G_1 is wind wheel gravity and G_2 is engine gravity. h is the eccentricity. By substituting the parameters of Table 4 to the calculation formula, the tower top load can be calculated and the results are listed in Table 5.

Table 5 Loads on the top of the tower

Load condition	F_x(kN)	F_y(kN)	F_z(kN)	M_x(kN·m)	M_y(kN·m)	M_z(kN·m)
Rated load	763.02	8.4	2077.6	4116	2376.5	282.29
Ultimate load	1261.67	27.81	2077.6	4116	3456.7	969.993
Storm load	1883.25	37.54	2077.6	4116	4704.09	1309.5

4.2 Wind load model

The standard value of the wind load on unit area can be calculated according to the structural load code (MHURD of PPC 2002). The standard value of wind load equals to 222.83 N/m^2 for the hybrid tower under rated wind load according to calculation.

5. THEORETICAL ANALYSIS OF MINIMUM SEGMENTAL THICKNESS

In the first step of preliminary analysis of the hybrid tower, the segment minimum thickness determination is a key issue. The UHPCC combined tower can be simplified as cantilever beam under shear, bending and torque. Here, for simplification, only combination of bending and compression theory of reinforced concrete column is used here. An influence coefficient will thereafter be used to consider toque affect in which only wind wheel torque M_z is taken into account. Since only the overall geometric design variables affects is focused on, segmental connections is assumed to be perfect.

Now, the minimum thickness is determined according to the bending and flexure circular column theory. The results are shown in Table 6. Indeed the circular cross section also exist shear stress caused by torque and horizontal shear force. Based on Mises effective stress analysis, a torque influence coefficient is defined to consider the influence of shear stress caused by torque. The influence coefficients corresponding to the thickness at different ratios of torque and moment are shown in Figure 5.

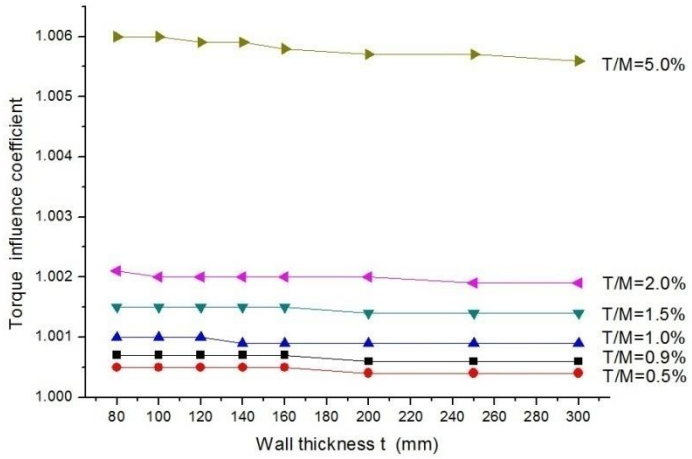

Figure 5 Variations of the torque influence coefficient and wall thickness

As can be seen from figure 5, the torque influence coefficient increases obviously with the torque-moment ratio increasing. When T/M≤5%, the coefficient η_t recommend as 1.01. According to the ultimate load analysis, the T/M of the hybrid tower is equals to 0.9%. On the basis of Table 6, the modification of the minimum design wall thickness are calculated and listed in the last column of Table 6.

Table 6 Minimum wall thickness at different heights under ultimate load

Height from special section to ground (mm)	Bending moment M(kN·m)	Axial force N(MN)	t (mm)	Adjusted value of t(mm)
0	1.64×10^5	3.64	13.5	14
2×10^4	1.37×10^5	2.89	41.2	42
4×10^4	1.09×10^5	2.58	37.0	38
6×10^4	8.22×10^5	2.34	31.8	33
8×10^4	5.55×10^5	2.21	19.7	20
10×10^4	2.94×10^5	2.13	12.9	14
12×10^4	5.38×10^3	2.08	8.57	9

According to the minimum design wall thickness analysis and constructive design conceptions, the minimum wall thickness of 100mm is selected initially. Thus, thickness combinations are the second key issue for the structure preliminary design, i.e. whether or not the wall thickness different combination has big influence on the structural behavior. Let bottom wall thickness is bigger than middle segments. Now, the wall thickness combination affects analysis is divided into two cases. Equal proportional thickness combination with constant ratio 2:3 and varied proportional thickness combination of 100-200, 200-300, 200-240 with varied ratios 3:6, 4:6, 5:6.

6. STRUCTURAL OVERALL ANALYSIS OF THE HYBRID TOWER

6.1 Finite element model

High strength steel wire with ultimate tensile strength 1860 N/mm^2, density of 7850 kg/m^3, linear expansion coefficient of 1.2635, modulus of 1.95e11, and Poisson's ratio of 0.3 is used for the prestressed tendon. The initial prestress is 1231MPa. ABAQUS/Standard Version 6.10-1 is used in this study. The concrete damaged plasticity model was used to model the UHPC while the classic metal plasticity model was used for modeling the tendon's material. The end of the tendon is embedded in the loading stub and the foundation to simulate the tendon's anchorage. The tendon is subjected to a stress type initial condition to simulate its post-tensioning. By neglecting the foundation sliding, the foundation bottom is constrained in the three directions.

Modeling of the tower was divided into seven parts， part1-4 are the bottom segments, Part5 is a segment in the middle, post-tensioning tendons were part6-7. The model was built up using 3D solid elements C3D4 for concrete and truss elements for the post-tensioning tendons. Two loading steps are used for the analysis of the models without boundary displacements in all directions. During the first step, a post-tension force is applied by using falling temperature method. The second step consisted of the gravity load, three directions concentrated force, bending moment on the top and wind load distribution along the vertical tower. Structured and sweep edges methods were used in meshing, because the size of the tower is too large. In order to analyze the overall structural behavior, tie binding was used between each tower segments to simulate the perfect connections.

6.2 Finite element results

The stress distribution and lateral displacement of the typical size UHPC hybrid wind turbine tower under the ultimate limited wind loads are calculated include the maximum stress of the windward side and the leeward side as shown in Table 7.

6.3 Result analysis

6.3.1 Affect of wall thickness combinations with constant ratio

When the wall thickness ratio of the upper and lower segments is constant (here typical 2/3 is used), the corresponding typical wall thickness combination are 200-300mm, 140-210mm, 100-120mm. The distribution of stress, strain and displacement along the tower are shown in figure 6 and figure 7.

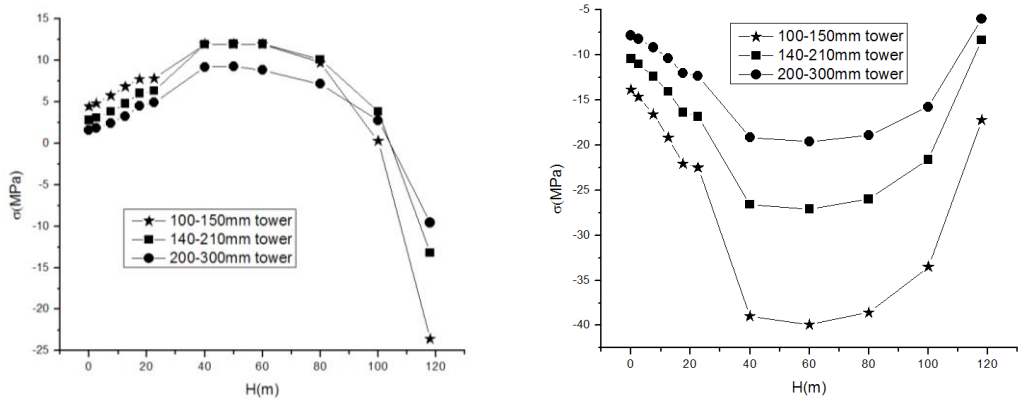

(a) Windward side (b) Leeward side

Figures 6 Stress distributions along the height

From Figure 6(a), it can be seen that UHPC tensile stress increases linearly in the range of basement 40m height of the tower with the height increasing. The tower stress converted to compress in the range of 100-120m height for the wall thickness combinations of 200-300mm and 140-210mm. The compressive stress on the top reaches maximum. For the wall thickness combination of 100-150mm, the tower stress variation is large. Tensile stress rapidly decreased at the height of 80m, turned to compressive stress at the height of 100m.

It can be seen from figure 6(b) that the leeward side of tower is mainly compression zone. Compressive stress increased with height increased during the range of previous 40m height. The compressive stress increased on this basis due to pre-stress. In the range of 40m to 100m, compressive stress variation is stable with a general trend of decrease. Compressive stresses reached the maximum at 60m height of the tower under the wall thickness combinations of 200-300mm, 140-210mm and 100-150mm. At the height of 100m, compressive stress decrease, and the curvature gradually decreased.

Table 7 Results the typical size tower under ultimate limit wind load

t(W-T) (mm)	Stress and disp.	Coordinate along the height of the hybrid tower from 0 to 118 meter											
		0	2.5	7.5	12.5	17.5	22.5	40	50	60	80	100	118
100-150	σ_w	4.45	4.81	5.75	6.85	7.75	7.83	11.99	11.99	11.99	9.72	0.31	-23.52
	σ_l	-13.86	-14.65	-16.57	-19.15	-22.07	-22.48	-39	-39.12	-39.92	-38.6	-33.49	-17.21
	U	0	0.41	2.68	4.54	11.2	11.13	72.78	126.83	397.51	675.51	1033.44	1511.15
100-200	σ_w	3.26	3.56	4.27	5.15	6.18	6.44	11.98	11.98	11.98	9.72	0.31	-23.57
	σ_l	-10.61	-11.19	-12.7	-14.64	-17.42	-18.12	-38.93	-38.95	-39.92	-38.59	-33.49	-17.21
	U	0	0.32	2.08	3.08	9.05	8.05	63.06	113.65	373.89	644.94	995.91	1465.95
140-210	σ_w	2.78	3.1	3.84	4.8	6.04	6.36	11.97	11.98	11.98	10.11	3.83	-13.18
	σ_l	-10.44	-10.98	-12.36	-14.06	-16.34	-16.81	-26.57	-26.6	-27.1	-25.96	-21.58	-8.35
	U	0	0.26	1.84	2.82	8.42	7.89	51.8	89.8	281.14	479.91	738.68	1086.13
200-240	σ_w	1.99	2.3	3	3.97	5.4	5.76	7.43	7.46	6.72	4.81	0.13	-12.67
	σ_l	-9.6	-10.09	-11.28	-12.82	-15.02	-15.49	-19.98	-20.1	-20.84	-20.52	-17.96	-9.19
	U	0	0.28	1.27	2.54	7.03	7.2	38.41	64.62	194.58	329.88	507.59	748.51
200-300	σ_w	1.57	1.83	2.44	3.26	4.52	4.92	9.21	9.3	8.83	7.15	2.76	-9.55
	σ_l	-7.83	-8.22	-9.16	-10.34	-11.99	-12.34	-19.16	-19.17	-19.61	-18.93	-15.75	-6.01
	U	0	0.21	1.1	1.94	6.15	5.78	36.25	62.59	195.35	334.6	517.8	766.04
200-300 (without pre-stress)	σ_w	3.43	3.51	4.56	5.3	6.7	7.06	11.98	12.25	12.44	11.38	7.86	-2.99
	σ_l	-9.46	-9.91	-11.09	-12.38	-14.17	-14.48	-22.33	-22.45	-23.15	-23.07	-20.85	-12.56
	U	0	0.07	0.93	1.55	6.18	5.87	36.26	62.89	195.65	334.89	518	766.44

It can be seen from figure 7 that the maximum displacement section of the tower is located at the top. The displacement increased with the increasing height of the tower, the longitudinal deformation of the structure was bending type. At first 50m of the tower, displacement variation was relatively flat. According to practical experience, the maximum allowable deformation is 0.5%～0.8% height of the tower. The maximum displacement of 200-300mm tower at the top was 0.638% of the tower height. The deformation of this tower was 0.76/120, about 1/150, within the limits. The maximum displacement of 140-210mm, 100-150mm tower exceeded the allowable deformation. Three different thicknesses tower displacement values were 334.59, 479.91 and 675.51 at 80m nodes. At 60m nodes, displacement values were 195.35, 281.14 and 397.51. The displacements at 100m values were 517.8, 738.68 and 1033.44. Displacement growth curve is linear.

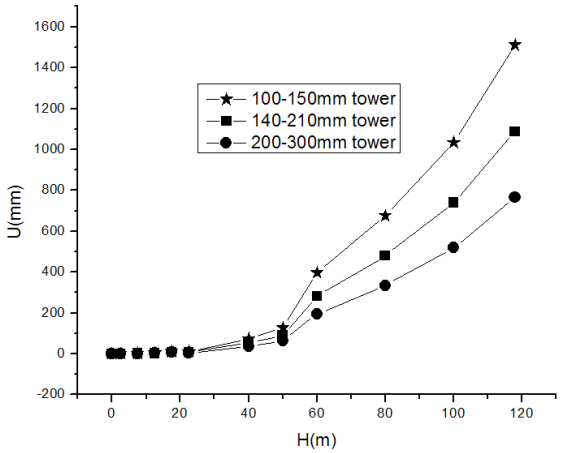

Figure 7 The displacement of three thicknesses tower under limited wind speed

6.3.2 Affect of wall thickness ratio on tower structural performance

Varied tower thickness ratios of 3:6, 4:6, 5:6 are considered here. Tower deformation and internal force distribution were shown in figure 8 and figure 9, and corresponding wall thickness were respectively 100-200mm, 200-300mm and 200-240mm.

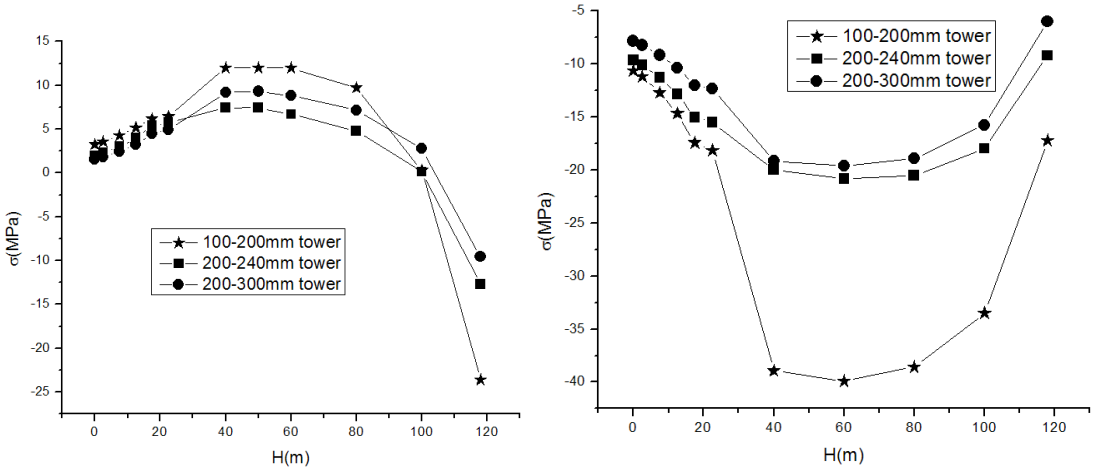

(a) windward side (b) Leeward side

Figure 8 Stress distribution of the tower under three different thickness ratios

It can be seen from figure 8 (a), the general variation trends are similar with the affect of wall thickness ratio. The structural response is more significant for wall thickness ratio 3:6. Tower compressive stress reached the maximum at the height of 60m. In the range of more than 100m height, the compressive stress began to decrease significantly. It can be seen from figure 8(b) in the cases of 4:6 and 5:6, the tower stress strain curve was relatively flat. However the stress of tower varies relatively large for thickness ratio of 3:6. The stress and strain changed greatly in the range of 20~40m, and the danger point locates at here.

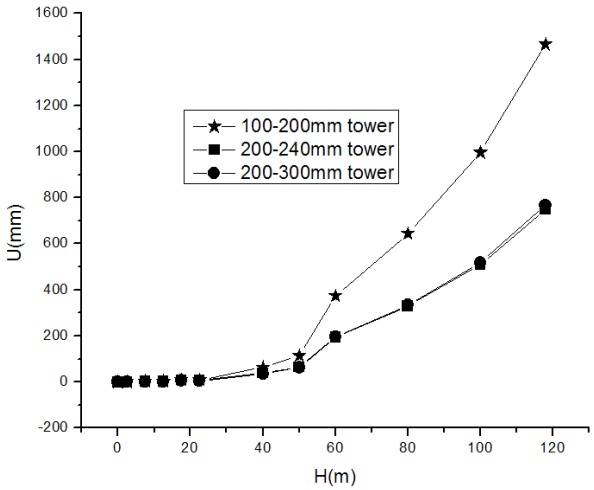

Figure 9 Displacement of three thicknesses ratios under ultimate speed

It can be seen from figure 9 that the maximum displacement of the tower was at the top. At 80m, the displacement of 200-300mm and 200-240mm tower increases linearly. The displacement of 100-200mm tower changed greatly, and it was non-linear growth. The displacement values of three different thicknesses were 334.6, 329.88 and 644.94 at 80m nodes. At 60m nodes, displacement values were 195.35, 194.58 and 373.89. At 100m nodes, the displacement values were 517.8, 507.6 and 995.9. The displacement growth curve is also nonlinear.

6.3.3 Affect of pre-stressing force

Considering the tower with wall thickness combination of 200-300mm, and the stress and displacement in both cases of pre-stress and without pre-stress are calculated as shown in figure 10 and figure 11.

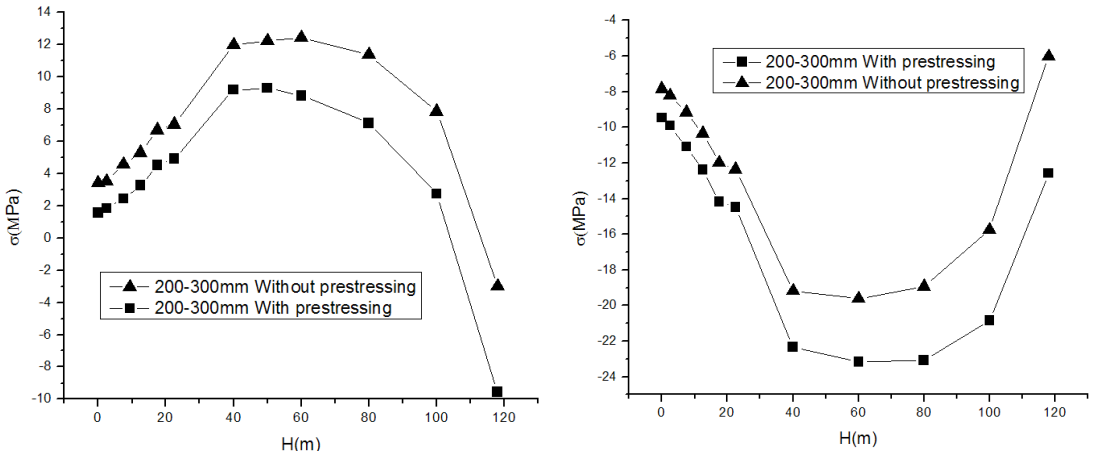

(a) windward side (b) Leeward side

Figure 10 Affect of pre-stress on stress distribution

The maximum tensile stress of the tower reaches to 12MPa for the case without pre-stress as shown in figure 10. Part of the tensile stress can offset by pre-stress. The maximum stress value reduces to 9MPa with prestressing action. The pre-stress can effectively reduce the stress of the tower and the tower had a better stability.

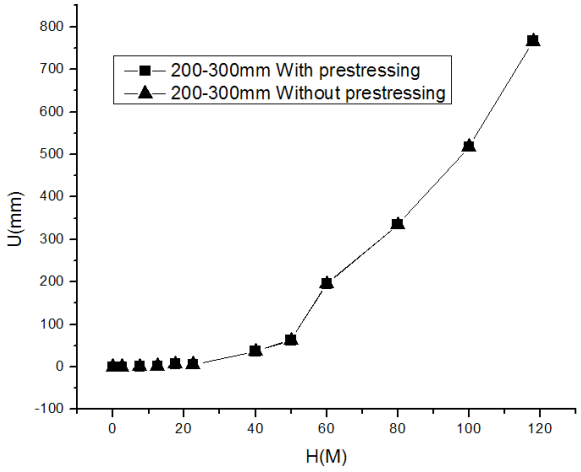

Figure 11 Affect of pre-stress on displacement

As can be seen from figure 11, the displacement curves of tower had little changes under both cases which indicates that pre-stress had little effect on tower displacement.

7. CONCLUSIONS

(1) In the typical case of wall thickness combination with constant ratio, longitudinal tension stress peak value is in the range of 30m-60m and close to the initial crack strength of UHPC-200. In the range of 100m-120m, total section of the segmental is compression zone. Wall thickness combination with constant ratio has little effect on

the displacement. With the decreasing of the middle segment, the displacement of middle node increases linearly.

(2) In the case of wall thickness combination with varied ratio, the stress and nodal displacement change continuously in the transition region of lower and middle section. The stress and displacement grows nonlinearly. In the middle segments, with the longitudinal node height increasing, the nodal displacements show non-linear growth. For engineering design, wall thickness combination with varied ratio is recommended no less than 2/3.

(3) Pre-stressing tendons had little effect on the node lateral displacement of lower and middle segments. According to the analysis, pre-stressing effect on the structural deformation is not obvious..

ACKNOWLEDGEMENTS

The authors would like to thank the China National Natural Science Fund (51008088), the fundamental Research Funds for the Central Universities (Grant No. HIT. NSRIF. 2013112), the project sponsored by Harbin city science and technology innovation talents special funds(2011RFLXG014), and Heilongjiang Province Natural Science Fund (E200911) for providing funding to this project, the Science and Technology project of Education Department of Heilongjiang Province for the support to the authors work described herein.

REFERENCES

Behloul, M. (2007), “HPFRCC field of applications: Ductal recent experience”, 5th High Performance Fiber Reinforced Cement Composite (HPFRCC5), Mainz, Germany, July, 2007.

Benjamin A. G. (2006), “Structural Behavior of Ultra-High Performance Concrete Prestressed I-Girders”. Report No. FHWA–HRT–06–115, Federal Highway Administration, Mclean, VA, August, 2006.

Brughuis F.J.(2004), “Improved return on investment due to larger wind turbines”. Mecal Applied Mechanics BV P.O. Box 286, 7500AG, Enschede the Netherlands, www.mecal.nl.

Cavill, B. and Chirgwin, G.. (2003), “The worlds first Ductal road bridge Sherpherds gully creek bridge, NSW”, 21st Biennial Conference of the Concrete Institute of Australia, Brisbane.

Eize de Vries. (2009), “Advanced Tower Systems (ATS) of the Netherlands inaugurated a prototype of its patented concrete–tubular steel hybrid tower concept at one of Germany’s wind turbine test fields”, near Grevenbroich, Renewable Energy World September-october 2009.

Graybeal, B., Hartamann, J., and Perry, V. (2004), “Ultra-high performance concrete for highway bridge”, FIB Symposium, Avignon, 26-28 April.

Kittinun S., Sherif E.T., and Gustavo P.M. (2010), “Behavior of high performance fiber reinforced cement composite under multi-axial compressive loading”, Cement & Concrete Composite, 32(2010): 62-72.

Ma L.H., Dai H.T., Zhang D.T., and Liu D.Y., (2008), “Design and Analysis for MW Wind Turbine Tower”, 2008 Annual Meeting of Clean & Efficient Coal Power Generation Technology Network, October 2008 Nanjing, China: 1-4.

Nesttor A. Agbayani, Rolando E. Vega.(2012), “The rapid evaluation of wind turbine tower structural systems: a historical and technical overview”. Proceedings of Structures Congress 2012(ASCE), Chicago, USA, Mar. 2012: 1201-1212.

Okuma, H., et al.(2006), “The first highway bridge applying ultra high strength fiber reinforced concrete in Japan”, 7th International Conference on short and medium span bridge. Montreal, Canada.

Ramadoss P. and Nagamani K. (2008), “A new strength model for the high-performance fiber reinforced concrete”, Computers and Concrete, 5(1): 21-36.

Staffan, E., Tomas L., Manouchehr H., Thomas S. and John J.(2010), “Tall towers for large wind turbins”, Report from Vindforsk project V-342 Höga torn för vindkraftverk : 3-10.

Tricklebank A., Bromage A., (2007), “Concrete Towers for Onshore Wind Farms” The Concrete Centre, www.concretecentre.com: 16-26.

The People's Republic of mechanical industry standard JB/T 100300-2001, Wind Turbine Generator system-Design Requirements, Beijing, 2001.

Wu X.G. and S.M. Han S.M., (2010), “Interface shear connection analysis of Ultrahigh-Performance fiber-Reinforced concrete composite girders”, J. of Bridge Engineering(ASCE), 15(5): 493-50.

Wu X.G., Zhao X.Y. and Han S.M. (2012), “Structural analysis of circular UHPCC form hybrid pier under construction loads”. Steel and Composite Structures, An International Journal, 12(2): 167-181

Williams E.M., Graham S.S., Akers S.A., Reed P.A. and Rushing T.S. (2010), “Constitutive property behavior of an ultra-high-performance concrete with and without steel fibers”, Computers and Concrete, 7(2): 191-202.

Zerous A. (2008), “Global development present situation and prospect of wind power”, China Energy, 30(4): 23-33.

Zhang W.L. (2009), “Research On Cone-shaped tower of MW grade wind turbine”, Shanxi University of Science and Technology, TM315: 15-22.

Zou L.H., Liang S.G., Li Q.S., Zhao L. and Ge Y.J.(2008), “Investigation of 3-D dynamic wind loads on lattice towers”, Wind and Structures, 11(4): 323-340.